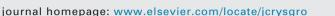
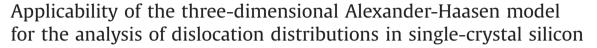


Contents lists available at ScienceDirect

Journal of Crystal Growth







CRYSTAL GROWTH

B. Gao^{a,*}, K. Jiptner^b, S. Nakano^a, H. Harada^b, Y. Miyamura^b, T. Sekiguchi^b, K. Kakimoto^a

^a Research Institute for Applied Mechanics, Kyushu University, Kasuga, Fukuoka 816-8580, Japan ^b National Institute for Materials Science, 1-1 Namiki, Tsukuba-city Ibaraki 305-0047, Japan

ARTICLE INFO

Article history: Received 8 October 2014 Received in revised form 4 November 2014 Accepted 5 November 2014 Available online 13 November 2014

Keywords: Computer simulation Line defects Stresses Semiconducting silicon

ABSTRACT

Applicability of the three-dimensional Alexander-Haasen (AH) model for the analysis of dislocation distributions in single-crystal silicon has been estimated. The numerical results obtained from the AH model agree well with the experimental data for both CZ-Si and FZ-Si crystals with the axis in the [001] direction but do not completely agree with the experimental data for the FZ-Si crystal with the axis in the [111] direction. The inapplicability of the AH model in a crystal with the axis in the [111] direction may arise from the neglect of dislocation propagation in this model, because the dislocation propagation in a crystal with the axis in the [111] direction. Therefore, to increase the applicability of the AH model, it is necessary to include the effect of dislocation propagation.

© 2014 Elsevier B.V. All rights reserved.

1. Introduction

Dislocations in crystalline silicon have been identified as one of the most relevant defect centers for efficiency of photovoltaic devices [1]. The demand for increased solar cell efficiencies necessitates a reduction in the number of dislocations. Both experiments and numerical simulations can be used to reveal how the number of dislocations can be reduced.

Experimental measurement is an important means for evaluating the final quality of crystalline silicon [2–5], but it has its limitations. Dislocations in silicon are usually activated in more than one slip system. Identifying the dislocations activated by every slip system in experiments is a challenging task. Furthermore, because the generation of dislocations occurs over a longterm crystal growth process, experimental work cannot identify the exact time and site at which the dislocations are generated during the growth, and thus cannot directly correlate the practical growth conditions to the final quality of crystal.

Numerical simulation provides an effective supplement for analyzing the final quality of the crystal. Many simulations have been done by using the advanced 3D Alexander-Haasen (AH) model [6–8], which considers multislip, immobilization of mobile dislocations, jog formation between the different slip systems and its influence on dislocation generation, and internal stress due to short-range interactions from the total dislocation density. Many valuable conclusions have been obtained by using this model. However, until now, there has been no evaluation of the applicability of this model. It is unclear whether it can be used for all types of single crystal silicon, and whether some limitations of this model exist.

Therefore, in this article we will focus on answering the following questions: Can the Alexander-Haasen model be used to describe the different type of single crystal silicon? If it cannot, what shortcoming of the model is the reason for this and how can the model be improved?

2. Evaluation process

To evaluate the AH model, two sets of experiments that used different types of single crystal silicon have been performed previously by another research [15]. The first set of experiments was performed on a CZ-Si crystal ingot with the axis in the [001] direction, while the second set of experiments was performed on a FZ-Si crystal ingot with the axis in the [111] direction. The two sets of experiments used the same heating and cooling processes. Thus, the differences between the two sets of experiments lie in crystal type and axis orientation.

For the most accurate comparison of the simulation and experimental results, numerical simulations must strictly follow the experimental operating conditions. To achieve this, a solver for the accurate control of the temperature history inside the simulated furnace was developed. Using this solver, two points on two

^{*} Corresponding author. Tel.: +81 92 583 7744; fax: +81 92 583 7743. *E-mail address:* gaobing@riam.kyushu-u.ac.jp (B. Gao).

heaters are monitored and the temperatures at the two monitored points are required to evolve according to a preset experimental curve. The details of the method can be found in Reference [9].

For completeness, first the AH model is briefly introduced, and then the experimental conditions are given.

2.1. Three-dimensional Alexander-Haasen model

The three-dimensional Alexander-Haasen model has been introduced in References [6–8]. Here, we present a brief overview of the formulas as follows.

Silicon crystal has an fcc structure that has twelve slip directions [9,10]. The resolved shear stress for each slip direction can be calculated from the tensor transformation technique using the stress components obtained from a three-dimensional analysis or an axisymmetric analysis [10]. After the resolved shear stress $\tau^{(\alpha)}$ in the α slip direction is obtained, the creep strain rate $d\varepsilon_{nl}^{(\alpha)}/dt$ is given by the Orowan relationship [11]:

$$\frac{d\boldsymbol{\varepsilon}_{pl}^{(\alpha)}}{dt} = N_m^{(\alpha)} \boldsymbol{v}^{(\alpha)} \boldsymbol{b},\tag{1}$$

where the subscript *m* denotes the mobile dislocation, the superscript α denotes the slip direction, b is the Burger's vector, N is the dislocation density, and v is the slip velocity of the dislocation.

The rate of the mobile dislocation density dN_m^{α}/dt in the slip direction α is given by

$$\frac{dN_m^{(\alpha)}}{dt} = KN_m^{(\alpha)}v^{(\alpha)}\tau_{eff}^{(\alpha)} + K^*N_m^{(\alpha)}v^{(\alpha)}\tau_{eff}^{(\alpha)}\sum_{\beta\neq\alpha}f_{\alpha\beta}N_m^{(\beta)} - 2r_cN_m^{(\alpha)}N_m^{(\alpha)}v^{(\alpha)},$$
(2)

where τ_{eff} is the effective stress for dislocation multiplication, *K* and K^* are the multiplication constants, r_c is an effective dipole half width, the $f_{\alpha\beta}$ coefficient is given a value of either one or zero according to whether a jog is formed on a screw dislocation of system α when cut by a forest dislocation of system β . On the right-hand side of Eq. (2), the first term models the dislocation increase due to the glide on the slip plane, the second term models the formation of jogs on a screw dislocation and the consequent expansion through spiral formation, and the third term models the sink for the mobile dislocation, i.e., immobilization. The values of *K*, K^* , and r_c were given in References [6–8].

For more clear understanding of Eq. (2), some physical explanations are needed. The first term on the right-hand side of Eq. (2)is based on the assumption that the increase in the length of dislocations in unit time is proportional to the area swept the mobile dislocations [13,14]; the second term is based on the assumption that the rate of formation of jogs is proportional to the number of times dislocations in different slip system cut each other, which can be modeled by a product of dislocation densities on the two slip systems [16]; the third term is based on the assumptions that mobile dislocation segments belonging to the same slip system and gliding on parallel planes can trap each other and form dipolar structures, and that rate of dipole formation is equal to the rate of immobilization of mobile dislocations [12].

The immobilization rate $dN_i^{(\alpha)}/dt$ is expressed as follows [12]:

$$dN_i^{(\alpha)}/dt = 2r_c N_m^{(\alpha)} N_m^{(\alpha)} v^{(\alpha)}.$$
(3)

The slip velocity of dislocation v is given by

$$v^{(\alpha)} = v_0 \left(\frac{\tau_{eff}^{(\alpha)}}{\tau_0}\right)^m \exp\left(-\frac{U}{k_b T}\right),\tag{4}$$

where $v_0 = 5000 \ m/s, \tau_0 = 1 \ MPa, \ m = 1$, and $U = 2.2 \ eV$ are used for crystal silicon [12]. The effective stress necessary for the dislocation motion is given by:

$$\tau_{eff}^{(\alpha)} = \left\langle \tau^{(\alpha)} - \tau_i^{(\alpha)} - \tau_b^{(\alpha)} \right\rangle,\tag{5}$$

where $\tau^{(\alpha)}$ is the resolved shear stress, $\tau^{(\alpha)}_i$ is the necessary stress for overcoming short-range obstacles, $\tau^{(\alpha)}_b$ is the internal longrange elastic stress generated by mobile dislocations [6-8,12], and $\langle x \rangle = x$ for x > 0, and zero for $x \le 0$.

The short-range internal stresses $\tau_i^{(\alpha)}$ emanates from the total dislocation densities defined by [12,17]

$$\tau_i^{(\alpha)} = \mu b \sqrt{\sum_{\beta} a_{\alpha\beta} (N_m^{(\beta)} + N_i^{(\beta)})},\tag{6}$$

with the coefficient $a_{\alpha\beta}$ given in references 12. The long-range internal stresses $\tau_b^{(\alpha)}$ emanates from mobile dislocations defined by [12,18]

$$\tau_b^{(\alpha)} = \mu b \sum_{\beta} A_{\alpha\beta} \sqrt{N_m^{(\beta)}},\tag{7}$$

where the coefficient $A_{\alpha\beta}$ is geometrically determined [18].

After dislocation densities and creep strains at all of the slip directions are solved, bethe total dislocation density and the total creep strain can be expressed as:

$$N_m = \sum_{\alpha = 1}^{12} N_m^{(\alpha)},$$
 (8)

$$\boldsymbol{\varepsilon}_{pl} = \sum_{\alpha=1}^{12} \boldsymbol{\varepsilon}_{pl}^{(\alpha)} \frac{1}{2} (\mathbf{n}^{(\alpha)} \otimes \mathbf{m}^{(\alpha)} + \mathbf{m}^{(\alpha)} \otimes \mathbf{n}^{(\alpha)}) sign(\tau^{(\alpha)}).$$
(9)

where $\mathbf{n}^{(\alpha)}$ and $\mathbf{m}^{(\alpha)}$ are the normal unit vector of the slip plane and the unit vector of the slip direction, respectively.

2.2. Operating conditions for experiments

Two sets of experiments were performed using an axisymmetric unidirectional solidification furnace. In the first experiment, a CZ-Si ingot with the axis in the [001] direction was used; whereas in the second experiment, an FZ-Si ingot with the axis in the [111] direction was used. Both crystals are axisymmetric and almost dislocation-free. The crystals were 90 mm in diameter and 80 mm in height. The diameter of the crucible was 96 mm. Thus, a small gap of 3 mm between the crystal and the crucible was maintained to avoid ambiguous boundary conditions between the crystal and the crucible. Furthermore, to avoid complexity, only the heating and cooling processes without solidification were used. The basic configuration of the furnace is described in Reference [9] and was described again for clarity (Fig. 1). The two monitoring points A and B are located on the top and side heaters, respectively.

To homogenize the temperature distribution inside the furnace, we required the temperature histories at the monitoring points A and B to be the same by automatically adjusting the two power settings on the top and side heaters. The preset temperature history (Fig. 2) must be followed by both simulation and experiment. In experiment, this can be realized by an automatic control technique, such as proportional-integral-differential (PID) control. In the simulation, a numerical solver that simulates the automatic control process has been developed for accurate control of the temperature history inside the furnace [9].

Fig. 2 shows the calculated temperature curves for points A and B. The calculated temperatures fit the preset temperature well except in the low-temperature region of the cooling process ($< 600 \degree$ C). The main reason for the difference between the designed and the calculated temperatures in the low-temperature region of the cooling process is that the temperature cannot linearly decrease Download English Version:

https://daneshyari.com/en/article/1790172

Download Persian Version:

https://daneshyari.com/article/1790172

Daneshyari.com